Commun. Theor. Phys. (Beijing, China) **32** (1999) pp 481–488

Vol. 32, No. 4, December 15, 1999

Spatiotemporal Chaos Control with Pinning Signals in Distributed Systems*

GAO JiHua,[1] XIAO JingHua,[1] YAO YiGui[2] and HU Gang[1]

[1]Department of Physics, Beijing Normal University, Beijing 100875, China

[2]LNM, Institute of Mechanics, The Chinese Academy of Sciences, Beijing 100080, China

(Received July 14, 1999)

Abstract *We suggest a local pinning feedback control for stabilizing periodic pattern in spatially extended systems. Analytical and numerical investigations of this method for a system described by the one-dimensional complex Ginzburg–Landau equation are carried out. We found that it is possible to suppress spatiotemporal chaos by using a few pinning signals in the presence of a large gradient force. Our analytical predictions well coincide with numerical observations.*

PACS numbers: 47.27.Rc, 05.45.+b
Key words: complex Ginzburg–Landau equation, spatiotemporal chaos, chaos control

I. Introduction

In the last half of twentieth century, chaos has been thoroughly investigated and well understood in many aspects, and become the central field in nonlinear science. Now, chaos application appears to be one of the most important tasks for further developing this field. In this respect, chaos control and synchronization are topics of most relevance. This is why after the pioneering works by Ott, Grebogi and York,[1] Pecora and Carroll,[2] Hubbler,[3] and Ditto *et al.*,[4] Roy *et al.*[5] for experiments, chaos control and synchronization have quickly attracted much attention.[6–10]

Recently, a great interest for chaos control and synchronization has been shifted to spatiotemporal systems[11–18] due to the following facts. First, turbulence and turbulence control remain among the extremely important problems in nature science for more than a century, and chaos control in spatiotemporal systems is directly aiming at the goal of turbulence control. Second, each chaotic spatiotemporal system is a reservoir of rich patterns (incomparably richer than nonchaotic systems), and the utilization of these patterns has great potential applications in wide fields, such as hydrodynamics, plasma physics, optics, and chemical reactions. Nevertheless, these applications can be realized only under the condition that spatiotemporal chaos or turbulence can be successfully controlled.

In this paper we take the complex Ginzburg–Landau equation (CGLE) as our model, and investigate its spatiotemporal chaos control both theoretically and analytically. In Sec. II, we introduce our model and control method. In Sec. III, we study the problems of controllability and control efficiency analytically. In Sec. IV, theoretical predictions are compared with numerical simulations, both coincide with each other. The last section gives a brief conclusion.

II. Model and Control Method

We consider the following CGLE

$$\partial_t A = A + (1 + \mathrm{i}c_1)\partial_x^2 A - (1 + \mathrm{i}c_2)\,|A|^2 A\,, \tag{1}$$

which appears universally in spatiotemporal systems around Hopf bifurcation condition. This equation serves as a typical model for studying pattern formation and turbulence, and has

*The project supported by the Foundation of the State Education Ministry of China for Doctoral Training

been investigated extensively in recent a few decades.[19–22] Here we generalize Eq. (1) to include a gradient term as

$$\partial_t A = A + r\partial_x A + (1 + \mathrm{i}c_1)\partial_x^2 A - (1 + \mathrm{i}c_2)\,|A|^2 A\,, \tag{2}$$

where the term of the first spatial derivative represents a drift force (bias), which can be very commonly observed in nature, e.g., in flows of charged particles under electrical fields or in hydrodynamic streams in sloping channels. The drift force is the key ingredient introducing convective instability and has been investigated thoroughly in open flow problems.[23,24] In this paper we will show that this entity is extremely important for controlling patterns and turbulence.

However, for period-boundary condition $A(L+x,t) = A(x,t)$ or for infinitely long systems, equation (2) is identical to Eq. (1) by the transformation

$$y = x - rt\,, \tag{3}$$

i.e., with any given initial condition $A(x, t = 0)$, the solution of Eq. (2) in the moving frame, $A(y,t)$, is exactly the same as that of Eq. (1) for $A(x,t)$. Equation (2) has travelling wave solutions

$$\begin{aligned} &A(x,t) = A_0 \exp[\mathrm{i}(kx - \omega t)]\,, \qquad && k = 2m\pi/L\,; \\ &A_0 = \sqrt{1-k^2}\,, && \omega = c_2 + (c_1 - c_2)k^2 - rk\,, \end{aligned} \tag{4}$$

where m is an integer or zero. The solutions (4) recover the solutions of conventional CGLE (1) for zero bias $r = 0$. As $1 + c_1c_2 < 0$ and for $L \gg 1$, all these solutions become unstable due to the well-known BF instability.[19] Note, the existence of the gradient force (nonzero r) does not give any influence to various instabilities, and then the BF curve is not affected by r due to the identity via the transformation (3). In the unstable region the system can show phase turbulence and defect turbulence.[19,22]

When the system is in a turbulence region, it is often desirable to kill turbulence and realize a certain stable ordered state, turbulence control is thus necessary. An effective approach for this purpose is to use local feedback control

$$\partial_t A = A + r\partial_x A + (1 + \mathrm{i}c_1)\partial_x^2 A - (1 + \mathrm{i}c_2)\,|A|^2 A + \varepsilon \sum_{i=1}^{N} \delta(x - x_i)[\bar{A}(x,t) - A]\,, \tag{5}$$

where $\bar{A}(x,t)$ is our ordered target state. Then the main idea of Eq. (5) is to inject signals, which are negatively proportional to the differences between the given state and the target regular state, to certain space points (pinnings). These injections first derive the system from the chaotic motions of the turbulence state to the target motions at these injected points and their vicinities, then bring the motion of the whole system to the target state through the space coupling. For sufficiently large ε the motions of injected points are expected to be pinned to the target state, then simple replacements of

$$A(x_i,t) = \bar{A}(x_i,t), \qquad i = 1,2,\cdots,m \tag{6}$$

are practically accepted. Therefore, for the simplicity of numerical simulation we can also directly use condition (6) as our control. Actually, the control (6) is nothing but boundary control, because the system evolution in the interval $x_i < x < x_{i+1}$ (we have $x_1 < x_2 < x_3 < \cdots < x_m$) is independent of the motions of all other regions $x < x_i$ and $x > x_{i+1}$, thus each part of $x_i < x < x_{i+1}$ can be actually regarded as an independent system and can be treated isolatedly with the periodic boundary conditions

$$\begin{aligned} &\partial_t A = r\partial_x A + (1 + \mathrm{i}c_1)\partial_x^2 A + (1 + \mathrm{i}c_2)(A - |A|^2 A)\,, \\ &A(x=0,t) = f_1(t), \qquad A(x=L,t) = f_2(t)\,. \end{aligned} \tag{7}$$

It is emphasized that the boundary control approach is convenient and practically applicable

in many realistic situations. For the theoretical analysis, we start from the general control scheme Eq. (5), and then recover the condition (7) in the limit $\varepsilon \to \infty$.

III. Theoretical Analysis on the Instability of Turbulence Control

To our knowledge, chaos control in continuous extended systems has been investigated only numerically up to date. In order to clearly understand the control mechanism and influences of various physical quantities on the control efficiency, it is absolutely necessary to have an analytical study on the problem. In this regard, the turbulence control in CGLE provides a perfect example. On one hand, the CGLE stems from realistic physical situations and presents typical turbulent state.[19–22] On the other hand, the CGLE is among very few examples accepting thorough analytic treatment for the problem of turbulence onset.

Suppose the system (2) is in a turbulence region, and a regular wave (4) $\bar{A}(x,t)$ exists and is unstable for the given parameters. Now we perform the control scheme (5), having $\bar{A}(x,t)$ as our target state. $\bar{A}(x,t)$ is certainly a solution of Eq. (5), the problem is whether $\bar{A}(x,t)$ can be stabilized by control. We consider a small deviation from the target state $\bar{A}(x,t) = A_0\,\mathrm{e}^{\mathrm{i}(kx-\omega t)}$,

$$A(x,t) = A_0[1 - a(x,t)]\exp\{\mathrm{i}[kx - \omega t + \phi(x,t)]\}\,, \tag{8}$$

and insert Eq. (8) to Eq. (5) and keep the linear terms of $a(x,t)$ and $\phi(x,t)$ only, a set of linearized equations can be reached

$$\begin{aligned} a_t &= a_{xx} + (r - 2kc_1)a_x - 2(1-k^2)a - c_1\phi_{xx} - 2k\phi_x - \varepsilon\delta(x)a\,,\\ \phi_t &= \phi_{xx} + (r - 2kc_1)\phi_x + c_1 a_{xx} + 2ka_x - 2c_2(1-k^2)a - \varepsilon\delta(x)\phi\,, \end{aligned} \tag{9}$$

where we denote

$$a_t = \frac{\partial a}{\partial t}\,, \qquad a_x = \frac{\partial a}{\partial x}\,, \qquad a_{xx} = \frac{\partial^2 a}{\partial x^2}$$

and so for ϕ_t, ϕ_x and ϕ_{xx}, and specify the values of A_0 and ω by Eq. (4). Assuming an eigenfunction of $\begin{pmatrix} a \\ \phi \end{pmatrix}$ corresponding to the eigenvalue σ, we can write the eigenfunction as

$$\begin{pmatrix} a \\ \phi \end{pmatrix} = \sum_{i=1}^{4} \begin{pmatrix} g_i \\ h_i \end{pmatrix} \mathrm{e}^{\sigma t}\,\mathrm{e}^{p_i x}, \tag{10}$$

where σ and p should be complex values as

$$\sigma = \lambda + \mathrm{i}\Omega, \qquad p_i = \mu_i + \mathrm{i}\nu_i, \qquad i = 1,2,3,4 \tag{11}$$

with all λ, Ω, μ_i, ν_i being real numbers. Three significant points of Eq. (10) should be remarked. First, σ is usually complex since equations (9) are non-Hermitian. Second, given an eigenvalue σ, there are four-mixing-waves to construct the corresponding eigenvector, since the eigen-equation (9) is a four-ordered ordinary differential equation. Third, the wave number $p_i\,, i = 1,2,3,4$, are usually complex too. The real parts μ_i characterize the behavior of convective instability. The last two points are interesting for characterizing the instability.

Two particular simplifications of Eqs (10) are worth while mentioned. Without control $\varepsilon = 0$, the eigenfunctions can be reduced to

$$\begin{pmatrix} a \\ \phi \end{pmatrix} = \begin{pmatrix} g \\ h \end{pmatrix} \mathrm{e}^{\sigma t}\,\mathrm{e}^{px}, \qquad p = \frac{2n\pi}{L}, \qquad n = 0, \pm 1, \pm 2, \cdots, \tag{12}$$

which are similar to those for $r = 0$,[21] since equations (1) and (2) are equivalent by the transformation (4).

In the case of $\varepsilon \neq 0$, $r = k = 0$, we can simplify Eq. (10) as

$$\begin{pmatrix} a \\ \phi \end{pmatrix} = \begin{pmatrix} g \\ h \end{pmatrix} \mathrm{e}^{\sigma t}\sin(px)\,. \tag{13}$$

In Eqs (12) and (13) we find only single wave at the instability (Re $(\sigma) = 0$). Therefore, four-mixing-wave eigenfunction exists only under the combined operations of both control and gradient bias (or a background wave).

Inserting Eq. (10) into Eqs (9) we obtain a set of two algebraic equations

$$\begin{aligned}\sigma g_i &= p_i^2 g_i + (r - 2kc_1)p_i g_i - 2(1-k^2)g_i - c_1 p_i^2 h_i - 2kp_i h_i\,,\\ \sigma h_i &= p_i^2 h_i + (r - 2kc_1)p_i h_i + c_1 p_i^2 g_i + 2kp_i g_i - 2c_2(1-k^2)g_i\end{aligned} \tag{14}$$

leading to the coefficient relations

$$h_i = \frac{p_i^2 + (r - 2kc_1)p_i - 2(1-k^2) - \sigma}{c_1 p_i^2 + 2kp_i} g_i\,, \qquad i = 1,2,3,4\,, \tag{15}$$

and the eigenvalue equations

$$\begin{aligned}&\sigma = \frac{1}{2}(F_{11}^{(i)} + F_{22}^{(i)}) + \frac{1}{2}\sqrt{(F_{11}^{(i)} + F_{22}^{(i)})^2 - 4(F_{11}^{(i)}F_{22}^{(i)} - F_{12}^{(i)}F_{21}^{(i)})}\,,\\ &F_{11}^{(i)} = p_i^2 + (r - 2kc_1)p_i - 2(1-k^2)\,, \quad F_{12}^{(i)} = -c_1 p_i^2 - 2kp_i\,,\\ &F_{21}^{(i)} = c_1 p_i^2 + 2kp_i - 2c_2(1-k^2)\,, \quad F_{22}^{(i)} = p_i^2 + (r - 2kc_1)p_i, \qquad i = 1,2,3,4.\end{aligned} \tag{16}$$

In Eqs (14) and (16) there are 12 complex unknown variables (with an arbitrary variable, say h_1, being excluded) for 8 complex equations. Then, the remained four free variables can be fixed by the boundary conditions at $x = 0$ and $x = L$, which are assumed to be pinned as in Eq. (5) (We consider a single pinning, the extension to multiple pinnings is direct),

$$\begin{aligned}&g(x=0,t) = g(x=L,t)\,, \qquad h(x=0,t) = h(x=L,t)\,,\\ &g_x(x=0,t) - g_x(x=L,t) - c_1 h_x(x=0,t) + c_1 h_x(x=L,t) = \varepsilon g(x=0,t),\\ &h_x(x=0,t) - h_x(x=L,t) + c_1 g_x(x=0,t) - c_1 g_x(x=L,t) = \varepsilon h(x=0,t),\end{aligned} \tag{17}$$

which yield

$$\begin{aligned}&\sum_{i=1}^{4} g_i = \sum_{i=1}^{4} g_i\,\mathrm{e}^{p_i L}\,, \qquad \sum_{i=1}^{4} h_i = \sum_{i=1}^{4} h_i\,\mathrm{e}^{p_i L}\,,\\ &\sum_{i=1}^{4}(g_i p_i - g_i p_i\,\mathrm{e}^{p_i L} - c_1 h_i p_i + c_1 h_i p_i\,\mathrm{e}^{p_i L}) = \varepsilon \sum_{i=1}^{4} g_i\,,\\ &\sum_{i=1}^{4}(h_i p_i - h_i p_i\,\mathrm{e}^{p_i L} + c_1 g_i p_i - c_1 g_i p_i\,\mathrm{e}^{p_i L}) = \varepsilon \sum_{i=1}^{4} h_i\,.\end{aligned} \tag{18}$$

Inserting Eq. (15) into Eq. (18) we obtain four homogeneous linear algebraic complex equations for four variables $g_i, i = 1,2,3,4$. In order that the equations have nonzero solution the corresponding determinant of coefficient matrix must vanish, this leads to

$$S(p_i, \sigma) = 0\,. \tag{19}$$

Combining Eqs (16) and (19) we have five complex equations for five unknown quantities σ and $p_i, i = 1,2,3,4$. Inserting the solutions of σ and p_i into Eqs (16) and (18) we can solve all coefficients $g_i, i = 2,3,4$ and $h_i, i = 1,2,3,4$ with g_1 being arbitrarily given. Therefore, the eigenvalue problem is solved completely and analytically. It is noticed that system (10) has an infinite number of eigenvalues and the corresponding eigenvectors. We are interested mostly in the eigenvalue and corresponding eigenfunction with the largest Re (σ), because this eigenvector determines the controllability of turbulence and the system behavior at the onset of instability.

IV. Comparison of Theoretical Predictions with Numerical Results

For having a general idea how the control can change the system stability, we plot the eigenvalue σ vs. the control strength ε in Fig. 1 for different r at $c_1 = 2.1$, $c_2 = -1.5$, $m = 2$

and $L = 100$ where the system is deeply in turbulence region. Since all equations (16) and (18) have real coefficients, if σ and p_i are the solutions of the equations, their conjugates σ^* and p_i^* must also be the solutions, which are not shown in Fig. 1. In Fig. 2 we do the same as Fig. 1 with eigenvalue σ replaced by the wave exponents p_i. From Figs 1 and 2, the following points are clear.

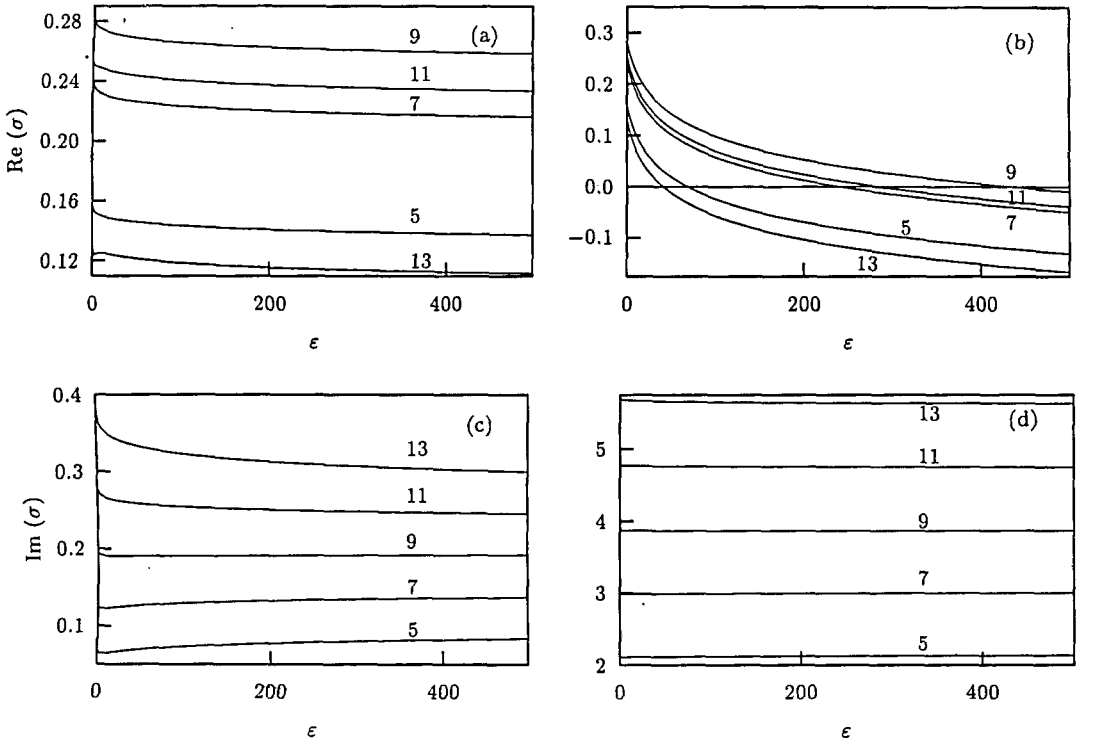

Fig. 1. $\sigma(n) = \lambda(n) + \mathrm{i}\Omega(n)$. (a) $\lambda(n)$ vs. ε with $r = 1.0$. (b) $\lambda(n)$ vs. ε with $r = 7.5$. (c) $\Omega(n)$ vs. ε with $r = 1.0$. (d) $\Omega(n)$ vs. ε with $r = 7.5$.

(i) Without control $\varepsilon = 0$, we always have a wave exponent (say p_1) equal to

$$p_1(n) = 0 + \mathrm{i}\frac{2n\pi}{L}, \qquad n = 0, \pm 1, \pm 2, \cdots . \tag{20}$$

[$\sigma(n)$ in Fig. 1 are labeled in the same order as Eqs (20)]. Then it is easy to verify the following identities

$$h_1, g_1 \neq 0, \qquad h_i = g_i = 0, \qquad i = 2, 3, 4. \tag{21}$$

The solutions (20) and (21) recover the known results (12), and the eigenfunction contains a single wave only at $\varepsilon = 0$.

(ii) By increasing ε from zero, p_1 deviates from Eq. (20), and $h_i, g_i, i = 2, 3, 4$ are no longer vanishing, then all four waves together build up the eigenfunctions.

(iii) As $\varepsilon \to \infty$, all eigenvalues saturate to certain values, which correspond to the solution of fixed boundary conditions

$$a(x = 0, t) = a(x = L, t) = \phi(x = 0, t) = \phi(x = L, t) = 0. \tag{22}$$

(iv) Among all $\lambda(n) = \mathrm{Re}(\sigma(n))$, there is a largest one, its turning point from positive to negative indicates the stability of the target state under control. For instance, for large gradient force $r = 7.5$, the target state can be stabilized (and then the turbulence can be controlled) after $\varepsilon > \varepsilon_c \approx 432$ (Fig. 1b); however, for small bias $r = 1$, the target state can never be stabilized whatever ε is taken (Fig. 1a).

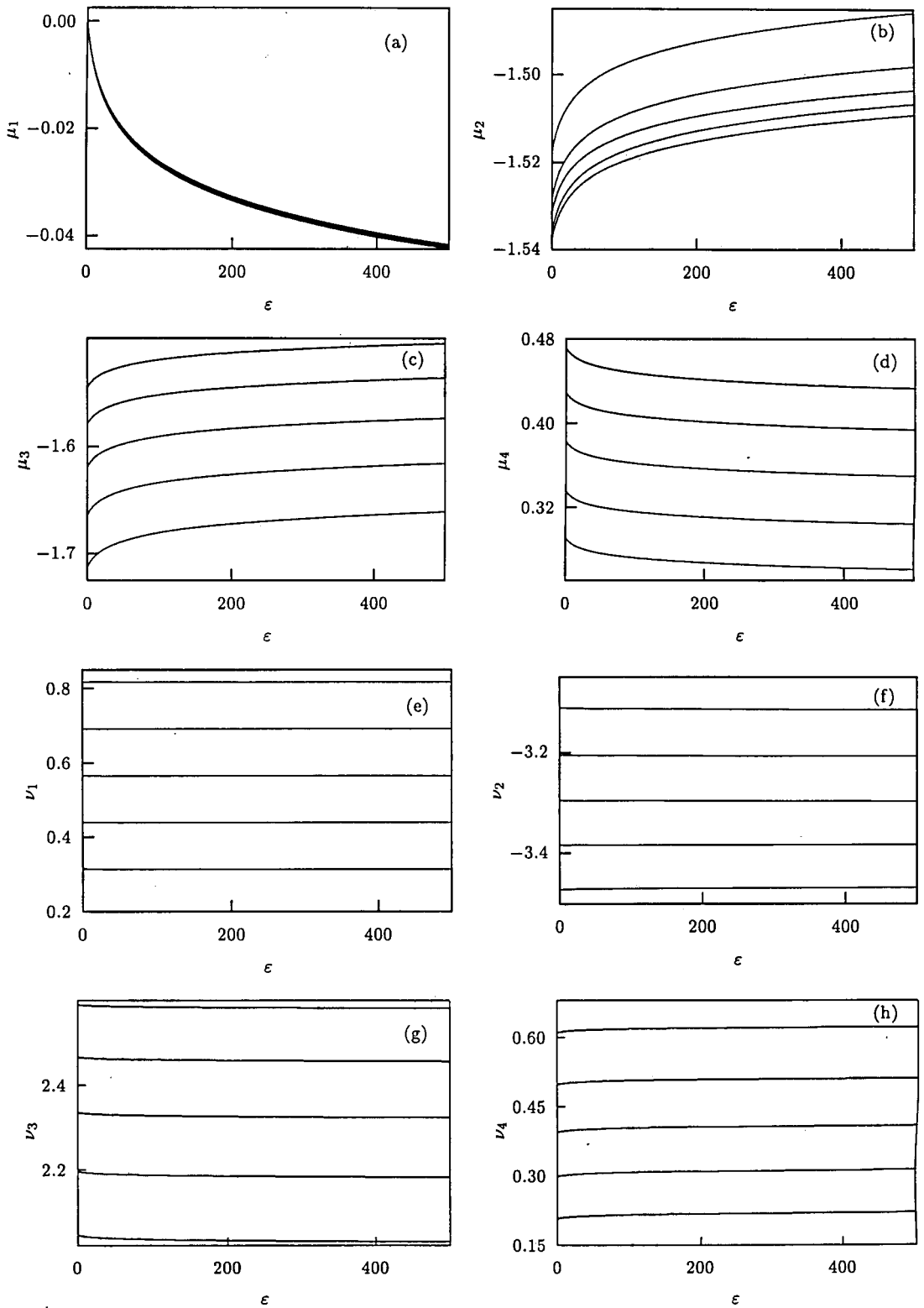

Fig. 2. $P_i(n) = \mu_i(n) + \mathrm{i}\nu_i(n)$. $r = 7.5$. (a) ~ (b) $\mu_i(n)$ vs. ε for $i = 1, 2, 3, 4$, respectively. (e) ~ (h) $\nu_i(n)$ vs. ε for $i = 1, 2, 3, 4$, respectively.

For comparing with the numerical simulation of Eqs (7), we consider $\varepsilon \to \infty$, and focus on Eqs (16) and (22). In Fig. 3 we plot $\sigma(n)$ vs. r for different L with other parameters being the same as Fig. 1. All the labels n come from Eqs (20) by continuously varying parameters. It is clearly shown that increasing r can definitely reduce $\mathrm{Re}(\sigma(n))$, and then is favorable to the stability of the target state, and then favorable to the turbulence control.

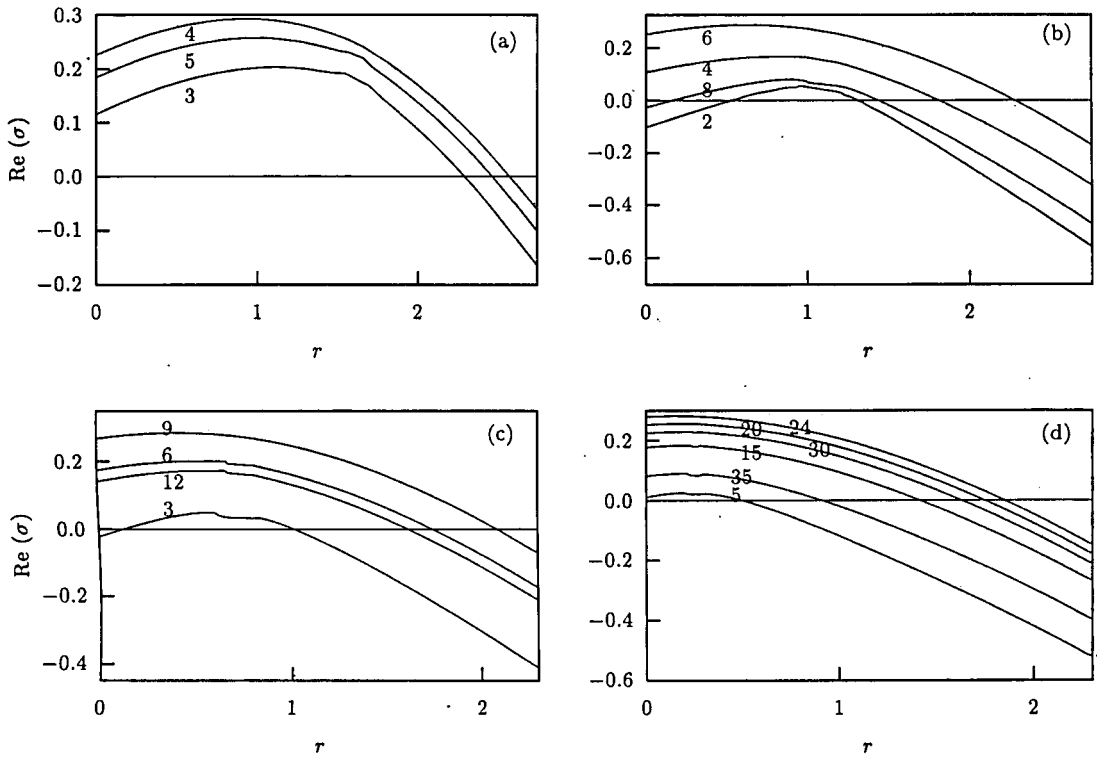

Fig. 3. $m = 2$, $\varepsilon \to \infty$, and the fixed boundary conditions (7) are used. (a) ~ (d) $\mathrm{Re}(\sigma(n))$ vs. r for L =40, 60, 90 and 256, respectively.

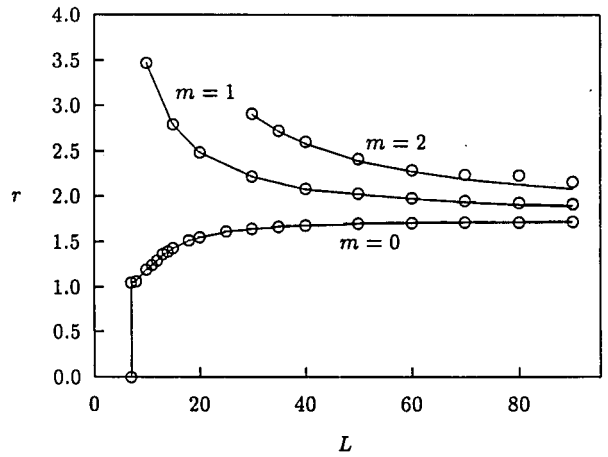

Fig. 4. r_c vs. L for different m. Target state can be stabilized and turbulence can be controlled in the regions above the curves. Solid lines are theoretical predictions from Eqs (16) and (22). Circles are obtained by running Eqs (7) from the initial condition $A(x,t=0) = \bar{A}(x,t=0) + \delta(x)$, $\delta(x)$ being randomly chosen in the interval $-0.01 < \delta(x) < 0.01$. Circles coincide with solid lines perfectly.

For having a more general point view on the controllability of the system, we plot r_c vs. L for different m at $c_1 = 2.1$ and $c_2 = -1.5$ in Fig. 4, where r_c is the lowest r for the stability of target state at the given L, and m is the wave number of the target travelling wave state of Eq. (4). Solid lines represent the theoretical predictions from Eqs (16) and (22). Circles indicate the results of numerical simulations of Eq. (7), starting from the vicinity $A(x, t = 0) = \bar{A}(x, t = 0) + \delta(x)$ with $\delta(x)$ being random number in the interval $-0.01 < \delta(x) < 0.01$. It is desirable that circles almost completely coincide with the solid lines.

V. Conclusion

In conclusion we would like to make the following remarks. We have performed successful turbulence control for turbulent states by applying pinning control and boundary driving approaches. Since any turbulent system is an extremely rich reservoir of infinitely many spatiotemporal patterns, successful turbulence control is of great significance for applications. The boundary control approach is convenient and practically realizable. The crucial condition for the high efficiency of turbulence control is the existence of sufficiently large drift force. It is emphasized that drift forces exist in nature very commonly. In certain cases turbulent systems do not contain drift force. It may still be possible to intentionally apply such drifts for realizing successful control. For instance, it is not difficult to apply uniform electrical or magnetic fields to the system if it consists of a charged medium.

References

[1] E. Ott, C. Grebogi and J.A. York, Phys. Rev. Lett. **64** (1990) 1196.
[2] L.M. Pecora and T.L. Carrol, Phys. Rev. Lett. **64** (1990) 821.
[3] A. Hubbler, Helv. Phys. Acta **62** (1989) 343.
[4] W.L. Ditto, S.N. Rauseo and M.L. Spano, Phys. Rev. Lett. **65** (1990) 3211.
[5] R. Roy, T.W. Maier, T.D. Gills and E.R. Hunt, Phys. Rev. Lett. **68** (1992) 1259.
[6] E.R. Hunt, Phys. Rev. Lett. **67** (1991) 1953.
[7] LIU WeiPing, YU DeJing and R.G. Harrison, Phys. Rev. Lett. **76** (1996) 3316.
[8] K. Pyragas, Phys. Lett. **A170** (1992) 421.
[9] G. CHEN and X. DONG, Int. J. Bifur. Chaos **2** (1992) 407.
[10] T. Kapitanik, Chaos, Solitons and Fractals **6** (1995) 237.
[11] G. HU and K.F. HE, Phys. Rev. Lett. **71** (1993) 3794.
[12] D. Auerbrach, Phys. Rev. Lett. **72** (1994) 1184.
[13] I. Aranson, H. Levine and L. Tsimring, Phys. Rev. Lett. **72** (1994) 2561.
[14] G. HU, Z.L. QU and K.F. HE, Int. J. Bifur. Chaos **5** (1995) 901.
[15] S. Mizokami, Y. Ohishi and H. Ohashi, Physica **A239** (1997) 227.
[16] L. Kocarev, P. Janginc, U. Parlitz and I. Stojanovki, Chaos, Solitons and Fractals **9** (1998) 283.
[17] J.H. XIAO, G. HU, J.Z. YANG and J.H. GAO, Phys. Rev. Lett. **81** (1998) 5552.
[18] Y. Kuramoto, *Chemical Oscillations, Waves and Turbulence*, Springer, New York (1984).
[19] M.C. Cross and P.C. Hohenberg, Rev. Mod. Phys. **65** (1993) 851.
[20] H. Chate and P. Manneville, Physica **A224** (1996) 348.
[21] B. Janiaud, A. Pumir, D. Bensimon and V. Croqutte, Physica **D55** (1992) 269.
[22] B. Shraiman, A. Pumir, W. Saarloos, P. Hohenburg, *et al.*, Physica **D57** (1992) 241.
[23] J.P. Cruthfield and K. Kaneko, *Directions in Chaos*, ed. by HAO BaiLin, World Scientific, Singapore (1990) p. 272.
[24] F.H. Willeboordse and K. Kaneko, Phys. Rev. Lett. **73** (1994) 533.